

# Rethinking Visual Token Reduction in LVLMs under Cross-modal Misalignment

Rui Xu<sup>1</sup>, Yunke Wang<sup>2</sup>, Yong Luo<sup>1</sup>, Bo Du<sup>1</sup>

<sup>1</sup>Wuhan University, <sup>2</sup>The University of Sydney  
 xurui7943@gmail.com, yunke.wang@sydney.edu.au, luoyong@whu.edu.cn, dubo@whu.edu.cn

## Abstract

Large Vision-Language Models (LVLMs) encode visual inputs as dense sequences of patch-level tokens to capture fine-grained semantics. These visual tokens often outnumber their textual counterparts by a large margin, leading to substantial computational overhead and limiting the scalability of LVLMs in practice. Previous efforts have explored visual token reduction either prior to or within the large language models (LLM). However, most in-LLM reduction approaches rely on text-conditioned interactions, implicitly assuming that textual tokens can reliably capture the importance of visual tokens. In this work, we revisit this assumption and reveal causal, semantic, and spatial forms of cross-modal misalignment. These misalignments undermine the effectiveness of text-guided visual token reduction. To address this, we introduce VisionDrop, a training-free, visual-only pruning framework that selects informative visual tokens based on intra-modal (visual-to-visual) attention, without relying on textual signals. To further suppress redundancy throughout the model hierarchy, we treat the visual encoder and the LLM as a unified system and design a progressive pruning pipeline. Our method performs dominant token selection and lightweight contextual merging at multiple stages, enabling fine-grained visual information to be retained even under aggressive token budgets. Extensive experiments across diverse benchmarks show that VisionDrop achieves consistent improvements over existing methods, despite requiring no additional training or complex modifications. Its simple yet effective design enables efficient inference while preserving strong performance across tasks.

## Introduction

Large Vision-Language Models (LVLMs) have achieved remarkable progress across a wide range of multimodal tasks (Liu et al. 2023; Li et al. 2024; Wang et al. 2024; Bai et al. 2025; Chen et al. 2025b; Zhu et al. 2025), such as visual question answering, image captioning, and visual reasoning. A key driver of this success is the use of dense patch-level tokenization, which encodes visual inputs as long sequences of tokens to capture rich fine-grained semantics. However, this dense representation comes at a significant computational cost. Compared to textual tokens, visual tokens often dominate the input sequence. It is common for a single image to be represented by hundreds or even thousands of tokens (Liu et al. 2024a), leading to quadratic growth in attention computation (Vaswani et al. 2017). This

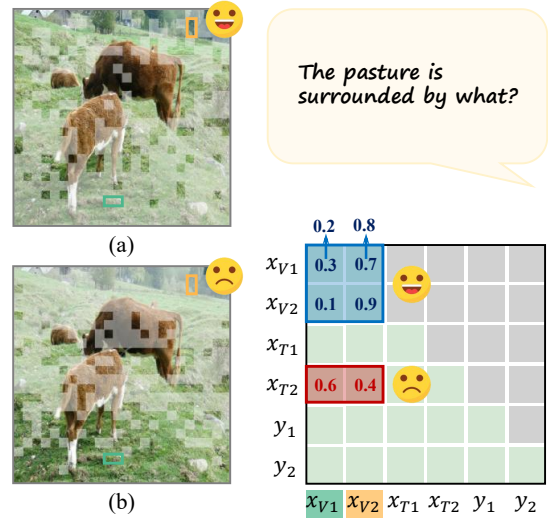


Figure 1: Comparison of visual token pruning strategies based on attention maps from the LLM decoding layers. Here,  $x_{V1}$  and  $x_{V2}$  denote visual tokens,  $x_{T1}$  and  $x_{T2}$  represent text instructions, and  $y_1$ ,  $y_2$  are autoregressively generated output tokens. (a) Our method identifies important visual tokens (e.g., the trees highlighted in orange) by leveraging image-to-image attention (blue box), which reflects intra-modal relevance and avoids interference from misaligned cross-modal signals. (b) In contrast, previous methods rely on image-to-text attention (red box) to assess visual token importance, which can be overly sensitive to cross-modal noise, resulting in the preservation of semantically redundant visual regions (e.g., the grass in green).

limits the scalability of LVLMs for high-resolution (Liu et al. 2024b) or real-time applications (Team et al. 2024).

To address this inefficiency, recent studies have explored reducing the number of visual tokens either before or within the layers of the large language models (LLM) (Yang et al. 2025; Zhang et al. 2025c; Chen et al. 2024b; Xing et al. 2025). Pruning visual tokens before entering the LLM enables effective compression of redundant features at the representation level, but may risk discarding subtle or task-relevant details. In contrast, performing token reduction

within the LLM allows uninformative tokens to be identified after visual information has been integrated into the language context, though it risks discarding entangled or contextually important features. Additionally, a more fundamental limitation of many in-LLM pruning strategies lies in their reliance on text-conditioned scoring mechanisms, which estimate the relevance between visual tokens and textual inputs. These approaches implicitly assume strong and persistent alignment between modalities throughout the LLM layers.

In this work, we revisit this critical assumption by asking: *Are visual and textual representations truly well-aligned within the LLM layers?* Our analysis uncovers three types of cross-modal misalignment that challenge this assumption and limit the effectiveness of text-guided visual token pruning: (1) Causal misalignment arises from the autoregressive nature of LLMs, where the last text token tends to focus on nearby tokens in the input sequence, introducing locality bias in visual token scoring. (2) Semantic misalignment emerges as visual and textual tokens become deeply entangled within LLM layers, weakening the distinctiveness and interpretability of textual queries for assessing visual importance. (3) Spatial misalignment stems from the flattening of positional embeddings across modalities and the absence of spatial priors in textual inputs. While visual encoders already struggle to align spatial structures with textual semantics, this issue worsens in the LLM, where visual and textual tokens are fused into a single sequence. Text-guided pruning under such conditions may discard spatially important regions that are not explicitly emphasized by the text. While CLIP-style encoders (Radford et al. 2021) and LVLM projection layers aim to align modalities at the input stage, such alignment degrades during multimodal token fusion in the LLM. As a result, pruning decisions based on text-guided signals may inadvertently discard visually salient or semantically important content.

To empirically validate this, we design a controlled study comparing visual-only and text-guided scoring strategies for visual token selection. Specifically, we replace image-to-text relevance scores with visual self-attention scores to assess the impact of modality alignment on pruning effectiveness across different compression ratios. Our findings reveal that, in general, visual-only scoring consistently outperforms text-guided scoring, especially under more aggressive pruning. This suggests that visual-textual alignment deteriorates as tokens propagate through the LLM, calling into question the reliability of text-guided reduction strategies.

Based on the analysis, we propose VisionDrop, a training-free framework for visual token reduction. Unlike prior approaches that rely on text-guided relevance, VisionDrop estimates token importance solely from visual self-attention, avoiding dependence on potentially misaligned textual cues. Our method performs stage-wise pruning across the full LVLM architecture, progressively reducing visual tokens in both the visual encoder and LLM layers. First, the dominant token selection identifies highly referenced visual tokens by the aforementioned visual-only importance score, ensuring that key semantic content is retained. Second, the lightweight contextual merging aggregates remaining tokens

into contextual tokens by similarity, preserving complementary information. Together, these components are applied at multiple stages in the model, allowing VisionDrop to maintain expressive visual representations even under tight token budgets.

The contributions of our work are summarized as follows:

- We empirically investigate the misalignment between visual and textual representations within LLM layers and offer insights to the visual token importance scoring.
- We propose VisionDrop, a training-free pruning framework that progressively prunes visual tokens across both the visual encoder and the LLM.
- We propose a visual-only scoring method for dominant token selection and apply the contextual token merging to preserve complementary information at each stage.

Extensive evaluations on nine standard benchmarks demonstrate that VisionDrop achieves superior performance compared to state-of-the-art token reduction methods.

## Related Works

### Large Vision-Language Models

The evolution of large vision-language models (LVLMs) has been driven by the impressive generalization and reasoning abilities of large language models (LLMs) (Touvron et al. 2023; Jiang et al. 2023; Bai et al. 2023; Qwen et al. 2025; Cai et al. 2024), extending their success to the multimodal domain. Recent LVLMs integrate visual and textual modalities by projecting visual inputs into token sequences compatible with language models (Liu et al. 2023; Li et al. 2024; Wang et al. 2024; Bai et al. 2025; Chen et al. 2025b; Zhu et al. 2025), enabling them to leverage the full capacity of LLMs. However, the information density in visual data is often much lower than in textual data, resulting in an excessive number of visual tokens. For instance, LLaVA-1.5 (Liu et al. 2024a) encodes a  $336 \times 336$  image into 576 tokens, while LLaVA-NeXT (Liu et al. 2024b) expands this to 2,880 tokens for high-resolution input. This issue becomes even more critical in video understanding tasks. For example, LongVA (Zhang et al. 2024) transforms 2,000 frames into more than 200K visual tokens, while LongVILA (Chen et al. 2025a) supports inputs exceeding 6,000 frames and produces over a million visual tokens. The inflated visual token sequences place heavy demands on computation and memory, motivating the need for effective token reduction strategies to improve scalability and efficiency across tasks.

### Visual Token Reduction in LVLMs

To mitigate the computational burden in LVLMs, recent studies have explored reducing the number of visual tokens. Existing approaches to visual token reduction are primarily applied either in the visual encoder or within the LLM. They typically use either text-guided or text-agnostic scoring strategies to determine token importance. **Visual encoder pruning** approaches perform token reduction before tokens are fed into the LLM. Some approaches rely solely on visual information: FlowCut (Tong et al. 2025) leverages token-level information flow across layers to identify and

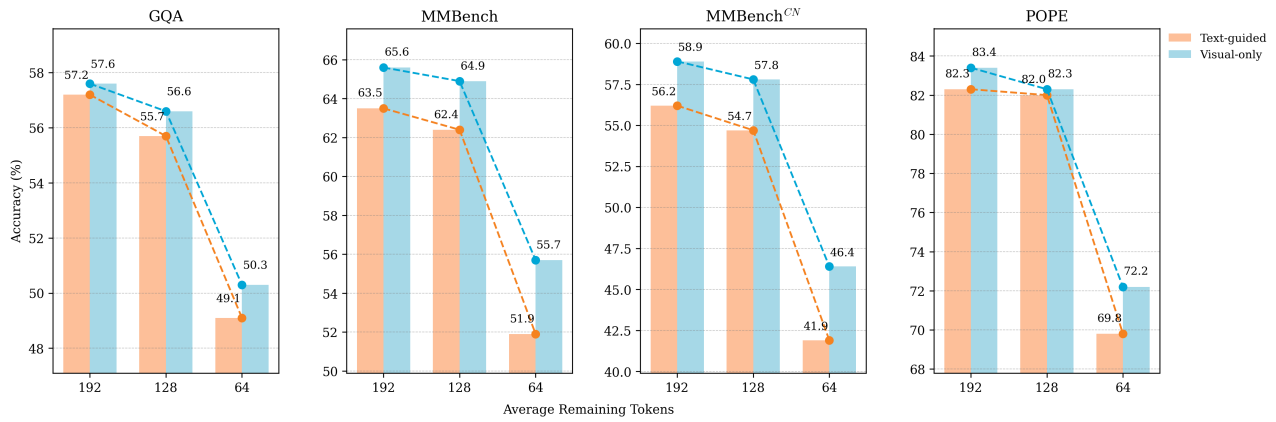


Figure 2: Accuracy comparisons between text-guided and visual-only scoring within LLMs across different average remaining token levels (192, 128, 64) on four benchmarks: GQA (Hudson and Manning 2019), MMBench (Liu et al. 2024c), MMBench<sup>CN</sup> (Liu et al. 2024c), and POPE (Li et al. 2023).



Figure 3: Visualization of text-guided visual token retention after shallow-layer pruning (specifically, the second layer) in the LLM. Pale translucent blocks indicate pruned tokens. Retained tokens consistently cluster at the bottom of the image, revealing a spatial bias caused by the causal attention in autoregressive LLMs.



Figure 4: Visualization of text-guided visual token retention at the end of the first three LLM stages. While the wallet-related region is correctly preserved in response to the first question, the model fails to retain relevant tokens around the umbrella in the second case, reflecting the semantic misalignment caused by modal entanglement in LLM layers.

prune redundant visual tokens in a progressive and structure-aware manner. VisionZip (Yang et al. 2025) selects dominant tokens based on attention scores and merges the rest

using semantic similarity. VScan (Zhang et al. 2025a) introduces a two-stage reduction pipeline by applying global-local scanning in the visual encoder pruning. Other works utilize textual guidance at this stage. CDPPruner (Zhang et al. 2025b) maximizes instruction-conditioned diversity of retained tokens. SparseVLM (Zhang et al. 2025c) computes token importance via cross-modal attention with text guidance. Although visual encoder pruning benefits from more structured token semantics, it may risk losing fine-grained cues critical for multimodal reasoning. **LLM decoding pruning** is an alternative direction that performs token reduction within the LLM, where visual and textual tokens are jointly processed. Most of these approaches adopt text-guided token selection. FastV (Chen et al. 2024b) ranks tokens based on their attention from text during generation, and VScan also extends its pruning into LLM layers based on cross-modal attentions. PyramidDrop (Xing et al. 2025) selects visual tokens that are most relevant to the final instruction token, performing progressive pruning across LLM layers. However, these approaches rely on the assumption that visual and textual tokens remain semantically aligned within the LLM, a property that is not guaranteed due to modality entanglement introduced by joint self-attention.

## Methodology

### Rethinking Text-guided Visual Token Reduction

To alleviate the computational overhead in LVLMs, recent studies have explored visual token reduction, either in the visual encoder (Yang et al. 2025; Zhang et al. 2025c) or during the LLM decoding phase (Chen et al. 2024b; Xing et al. 2025). In the latter case, mainstream approaches typically adopt text-guided strategies, using text relevance scores to determine which visual tokens to retain. However, this raises a critical question: *Are visual and textual representations truly well-aligned within the LLM layers?* Although visual inputs are projected into the textual embedding space before entering the LLM, using text-guided strategies for visual token reduction introduces three forms of **cross-modal mis-**

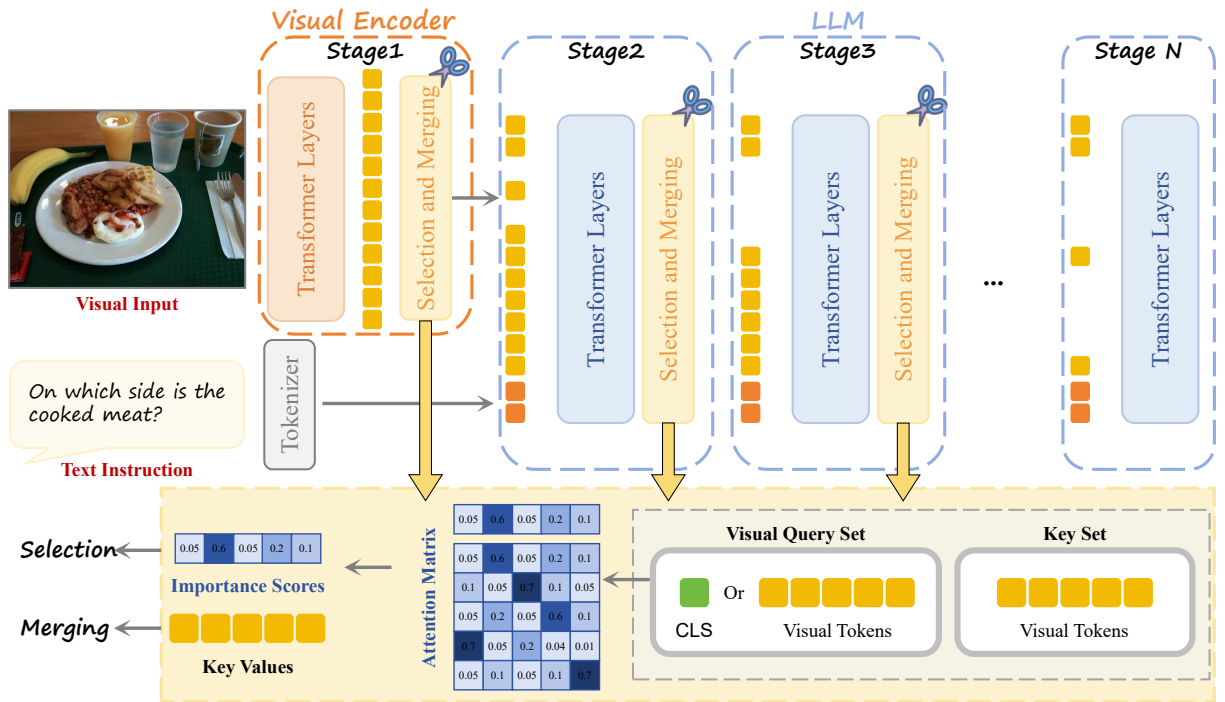


Figure 5: The visual encoder and LLM are partitioned into multiple pruning stages (e.g., Stage 1–N), where the number of visual tokens is progressively reduced. At the end of each stage, the importance of visual tokens is estimated via attention-based scores (bottom), computed from self-attention among visual tokens (optionally utilizing the [CLS] as the query). Low-importance tokens are merged with each other using key-value similarity to form contextual representations, which are then propagated together with informative tokens to the next stage.

**alignment**, due to the modality-specific biases in how visual and textual information are processed.

**Causal.** In text-guided pruning, the last text instruction token is commonly used to assess the importance of visual tokens. However, due to the causal nature of autoregressive LLMs, this token tends to focus disproportionately on later-positioned visual tokens in the input sequence (Zhang et al. 2025a). Unlike the [CLS] token or average-pooled visual features in bidirectional encoders, the instruction token does not serve as an explicit global aggregator. Figure 3 demonstrates this issue, where shallow-layer pruning results show that the retained visual tokens consistently cluster near the end of the input sequence, regardless of their semantic relevance.

**Semantic.** As tokens propagate through the LLM, visual and textual representations become increasingly entangled. The final instruction token evolves into a hybrid embedding that no longer maintains a clear semantic alignment with individual visual tokens, limiting its effectiveness in identifying visually important regions. This misalignment is evident in Figure 4, where the retained visual tokens often fail to correspond to the semantics of the input question.

**Spatial.** Preserving spatially relevant visual information has long been a challenge in LVLMs (Chen et al. 2024a). Even before entering the LLM, visual encoders (e.g., CLIP-style models (Radford et al. 2021)) often struggle to align

spatial structures with textual semantics, especially for tasks requiring fine-grained or spatial reasoning. This issue is further exacerbated within LLMs, where visual and textual tokens are flattened into a single sequence, and positional embeddings across modalities are merged, diluting the spatial priors of visual tokens. Moreover, textual inputs themselves lack spatial awareness and provide inherently incomplete representations of visual scenes. As a result, text-guided visual token pruning may amplify this spatial misalignment by discarding visually important regions that are not explicitly emphasized by the textual instruction.

These misalignments reveal that text-guided visual token pruning is fundamentally constrained by modality interaction biases. To empirically verify this, we conduct a controlled experiment by replacing text-guided scoring with visual-only scoring and observe the resulting performance changes. Specifically, we reproduce the PyramidDrop (Xing et al. 2025) framework. To ensure a fair comparison, we retain the same pruning configuration, including the pruning layers and token retention ratios, and replace the image-to-text relevance scores with image-to-image self-attention scores, thereby eliminating explicit textual guidance. We adopt LLaVA-v1.5-7B (Liu et al. 2024a) as the base LVLM and conduct extensive evaluations on 4 standard image understanding benchmarks, including GQA (Hudson and Manning 2019), MMBench (Liu et al. 2024c), MMBench<sup>CN</sup> (Liu et al. 2024c), and POPE (Li et al. 2023), to compare the ef-

fectiveness of the two scoring strategies. As shown in Figure 2, the image-only scoring strategy consistently outperforms the text-guided approach when retaining 192 visual tokens, and in general, the performance gap widens as the number of retained tokens decreases to 128 and 64. This performance gap under higher compression ratios indicates that visual and textual tokens are not well aligned within the LLM. Consequently, text-guided scoring, which implicitly assumes reliable cross-modal alignment, becomes increasingly unreliable when fewer visual tokens remain. In contrast, visual-only scoring exhibits greater robustness under aggressive pruning, highlighting its potential as a more stable and generalizable strategy for visual token reduction.

## Preliminaries

LVLMs are commonly structured with three components: a vision encoder, a modality projector, and an LLM. Upon receiving the visual input, the vision encoder extracts patch-level features, which are subsequently mapped into a set of  $n$  visual tokens  $\mathbf{x}_V = \{x_V^i\}_{i=1}^n$  via the projector. These visual tokens are concatenated with the tokenized textual tokens  $\mathbf{x}_T$  and fed into the LLM for autoregressive generation. At each timestep  $t$ , the model predicts the next token  $y_t$  based on the conditional probability  $p_\theta(y_t | \mathbf{x}_V, \mathbf{x}_T, \mathbf{y} < t)$ , where  $\mathbf{y} < t$  denotes the previously generated tokens.

## VisionDrop

Visual token reduction in LVLMs has been explored at two primary stages: either within the visual encoder (Yang et al. 2025; Zhang et al. 2025c) or during the LLM decoding phase (Chen et al. 2024b; Xing et al. 2025). We observe that pruning at the encoder stage tends to be more stable, as visual tokens remain semantically coherent and well-structured. However, this may lead to the loss of fine-grained visual details that are crucial for downstream reasoning. On the other hand, pruning in the LLM benefits from earlier visual-textual integration, where key visual cues may already be embedded in textual tokens, allowing more informed reduction. Yet as tokens propagate through the LLM layers, visual information becomes increasingly entangled and diffused, making it difficult to reliably estimate token importance.

To address the cross-modal misalignment within LLMs and to leverage the complementary strengths of different pruning stages, we propose a training-free, visual-only pruning framework that performs progressive visual token reduction at both the encoder and LLM stages, balancing stability and expressiveness across the model hierarchy.

**Progressive Dominant Token Selection.** We partition the LVLm architecture into a sequence of stages  $\mathcal{S} = s_0, s_1, \dots, s_N$ , including both the visual encoder and layers in the LLM decoder. At the end of each stage  $s_n$ , where  $n = 1, 2, \dots, N$ , we apply a stage-specific pruning ratio  $\lambda_n$  to the current set of visual tokens  $\mathbf{x}_V^{(s_n)}$ , where  $|\mathbf{x}_V^{(s_n)}| = \lambda_n \cdot |\mathbf{x}_V|$ . Tokens are ranked based on visual-only attention scores, and the top-ranked subset is propagated to the next stage  $s_{n+1}$ . The selection is given by:

$$\mathbf{x}_V^{(s_{n+1})} = \left\{ x_V^i \in \mathbf{x}_V^{(s_n)} \mid S(i) \geq \tau_n \right\}, \quad (1)$$

where  $S(i)$  denotes the visual importance score of token  $x_V^i$ , and  $\tau_n$  is a threshold determined by  $\lambda_n$ .

To identify the most informative visual tokens, we compute attention-based importance scores by reusing the model’s self-attention maps. Specifically, we measure how frequently each token is attended to by visual query tokens, averaged over all query positions. For clarity, we present the single-head attention formulation and omit the pruning stage notation.

Formally, let  $\mathbf{x}_V^q \in \mathbb{R}^{L_1 \times D}$  denote the set of query visual tokens, and  $\mathbf{x} \in \mathbb{R}^{L_2 \times D}$  be the full input sequence, including both visual and textual tokens. The attention query and key matrices are computed as:

$$\mathbf{Q} = \mathbf{x}_V^q \mathbf{W}_Q, \quad \mathbf{K} = \mathbf{x} \mathbf{W}_K, \quad (2)$$

where  $\mathbf{W}_Q, \mathbf{W}_K \in \mathbb{R}^{D \times D}$  are the projection matrices. The single-head attention matrix is obtained by:

$$\mathbf{A} = \text{Softmax} \left( \frac{\mathbf{Q} \mathbf{K}^\top}{\sqrt{D}} \right), \quad (3)$$

where  $\mathbf{A} \in \mathbb{R}^{L_1 \times L_2}$  contains attention scores from each query visual token to all tokens in the sequence.

To compute the final importance score  $\mathbf{S} \in \mathbb{R}^{L_1}$  over the visual tokens, we first extract the attention weights  $\mathbf{A}_{:, \mathcal{V}} \in \mathbb{R}^{L_1 \times L_V}$  corresponding to the visual key tokens from the full attention matrix  $\mathbf{A} \in \mathbb{R}^{L_1 \times L_2}$ . We then average across all visual queries:

$$\mathbf{S} = \frac{1}{L_1} \sum_{l=1}^{L_1} \mathbf{A}[l, \mathcal{V}], \quad (4)$$

where  $\mathcal{V}$  denotes the index set of visual tokens within the sequence.

*Visual Query Selection.* In the LLM, where no explicit [CLS] token exists, we compute visual-to-visual attention by isolating attention maps within the visual subspace. Specifically, we extract attention scores from image queries to the full token sequence, where  $\mathbf{Q}_V = \mathbf{x}_V \mathbf{W}_Q$  and  $\mathbf{K} = \mathbf{x} \mathbf{W}_K$ . We then retain only the entries in  $\mathbf{A}$  that attend to visual token indices.

In the visual encoder, if a dedicated [CLS] token is present (e.g., CLIP (Radford et al. 2021)), we use the attention from it to each visual token as the token importance, where  $\mathbf{Q}_{\text{CLS}} = \mathbf{x}_{\text{CLS}} \mathbf{W}_Q$ . If no such token exists (e.g., SigLIP (Zhai et al. 2023)), we follow a consistent strategy with the LLM and average the attention each token receives from all visual tokens.

This unified formulation allows our method to estimate token importance in a modality-consistent and architecture-adaptive manner.

**Stage-wise Contextual Token Merging.** While dominant tokens capture the primary visual content, discarding the remaining ones may result in missing subtle or auxiliary visual cues. To address this, we introduce a lightweight merging

Table 1: Performance comparison of vision-language models under different token retention rates.

Method	GQA	MMB	MMB <sup>CN</sup>	MME	POPE	SQA	VQA <sup>v2</sup>	VQA <sup>Text</sup>	VizWiz	Avg.
<i>Upper Bound, 576 Tokens (100%)</i>										
Vanilla	61.9	64.7	58.1	1862	85.9	69.5	78.5	58.2	50.0	100%
<i>Retain 192 Tokens (↓66.7%)</i>										
ToMe (ICLR23)	54.3	60.5	-	1563	72.4	65.2	68.0	52.1	-	88.49%
FastV (ECCV24)	52.7	61.2	57.0	1612	64.8	67.3	67.1	52.5	50.8	90.44%
PDrop* (CVPR25)	57.20	63.51	56.22	1783	82.31	<b>69.56</b>	75.59	56.1	48.9	96.61%
VisionZip* (CVPR25)	59.25	64.46	57.29	1767	86.39	68.86	76.78	57.26	<b>51.55</b>	98.64%
SparseVLM (ICML25)	59.5	64.1	-	1787	85.3	68.7	-	<b>57.8</b>	-	98.11%
VisionDrop (Ours)	<b>60.05</b>	<b>65.02</b>	<b>58.86</b>	<b>1788</b>	<b>86.83</b>	68.52	<b>77.21</b>	57.65	50.15	<b>99.14%</b>
<i>Retain 128 Tokens (↓77.8%)</i>										
ToMe (ICLR23)	52.4	53.3	-	1343	62.8	59.6	63.0	49.1	-	80.38%
FastV (ECCV24)	49.6	56.1	56.4	1490	59.6	60.2	61.8	50.6	51.3	85.36%
PDrop* (CVPR25)	55.65	62.39	54.71	1662	82.01	<b>69.66</b>	74.21	55.14	48.49	94.64%
VisionZip* (CVPR25)	57.62	63.40	56.67	1768	84.69	68.82	75.6	56.81	<b>52.02</b>	97.68%
SparseVLM (ICML25)	58.4	64.5	-	1746	85.0	68.6	-	56.7	-	97.15%
VisionDrop (Ours)	<b>58.65</b>	<b>65.02</b>	<b>56.84</b>	<b>1770</b>	<b>85.88</b>	68.72	<b>76.09</b>	<b>56.89</b>	51.2	<b>98.23%</b>
<i>Retain 64 Tokens (↓88.9%)</i>										
ToMe (ICLR23)	48.6	43.7	-	1138	52.5	50.0	57.1	45.3	-	70.11%
FastV (ECCV24)	46.1	48.0	52.7	1256	48.0	51.1	55.0	47.8	50.8	77.24%
PDrop* (CVPR25)	49.09	51.91	41.87	1427	69.75	68.27	63.7	49.56	50.66	83.92%
VisionZip* (CVPR25)	55.16	62.61	54.20	1687	80.45	69.01	72.42	55.48	<b>52.94</b>	95.13%
SparseVLM (ICML25)	53.8	60.1	-	1589	77.5	<b>69.8</b>	-	53.4	-	91.26%
VisionDrop (Ours)	<b>55.89</b>	<b>62.95</b>	<b>55.10</b>	<b>1698</b>	<b>81.58</b>	69.31	<b>73.16</b>	<b>55.59</b>	52.28	<b>95.73%</b>

step at each pruning stage to preserve such complementary information. While similar ideas have been proposed in prior work (Yang et al. 2025), our framework uniquely generalizes this operation across both the visual encoder and LLM decoder stages in a progressive fashion.

Specifically, we reuse the key embeddings from the attention module, which encode semantic content of tokens, to measure pairwise similarity. In the LLM, we explicitly extract the image-token portion of the key vectors before similarity computation, ensuring modality-pure merging. At the end of each stage, the non-dominant tokens are divided into candidate and reference sets, and each candidate token is matched to its most similar reference token based on a dot-product similarity. The matched tokens are then fused to produce enriched contextual tokens. This process ensures that visually redundant tokens are merged rather than dropped, preserving fine-grained details while keeping the token count under control.

## Experiments

### Image Understanding

**Models and Baselines.** We apply our proposed VisionDrop to the widely adopted LLaVA-1.5-7B (Liu et al. 2024b) model, and compare our method against several state-of-the-art visual token reduction baselines, including ToMe (Bolya et al. 2023), FastV (Chen et al. 2024b), Pyra-

midDrop (Xing et al. 2025), VisionZip (Yang et al. 2025), and SparseVLM (Zhang et al. 2025c).

**Benchmarks.** We evaluate our method on 9 standard image understanding benchmarks. These include general-purpose visual question answering datasets such as GQA (Hudson and Manning 2019), VQA<sup>v2</sup> (Goyal et al. 2017), and TextVQA (Singh et al. 2019); robustness and fairness benchmarks including POPE (Li et al. 2023), MM-Bench (Liu et al. 2024c), MMBench-CN (Liu et al. 2024c), and MME (Fu et al. 2024); as well as specialized datasets like VizWiz (Gurari et al. 2018), which features low-quality images captured by visually impaired users, and ScienceQA (SQA) (Lu et al. 2022), which focuses on scientific reasoning over visual inputs.

**Implementation Details.** We adopt the standard inference settings provided in the official implementations of each LVLM. For progressive visual token pruning, we divide the model into five stages: the first stage concludes at the output of the visual encoder, while the remaining four end at decoding layers  $l = 8, 16, 24$ , and the final decoding layer of the LLM. The number of visual tokens is gradually reduced across these stages. In the first stage, all original visual tokens are retained. For each target configuration—corresponding to a final token count of 192, 128, or 64—we set the retention number in the second stage to be  $1.5\times$  the final count, and prune proportionally in subsequent

Table 2: Ablation study on module combinations using LLaVA-1.5-7B with an average reduction rate of 22.2% on POPE and VQA<sup>Text</sup>.  $\Delta$  denotes improvement over the baseline.

V-only	Merge	Enc-Prune	GQA	POPE
			55.65	82.01
✓			56.57 (+ $\Delta$ 0.92)	82.33 (+ $\Delta$ 0.32)
✓	✓		56.94 (+ $\Delta$ 1.29)	83.18 (+ $\Delta$ 1.17)
✓		✓	58.55 (+ $\Delta$ 2.90)	85.79 (+ $\Delta$ 3.78)
✓	✓	✓	<b>58.65</b> (+ $\Delta$ 3.00)	<b>85.88</b> (+ $\Delta$ 3.87)

stages to meet the overall budget.

**Results.** As shown in Table 1, VisionDrop consistently outperforms all competing methods across different token retention levels. Even under an extreme compression setting that retains only 64 visual tokens (an 88.9% reduction), VisionDrop maintains 95.73% of the full-token performance, demonstrating strong efficiency with minimal degradation. Moreover, our method exhibits greater robustness as the pruning ratio increases. This is evidenced by the growing performance margin over the second-best method, VisionZip (Yang et al. 2025), especially at lower token counts. Although VisionZip performs relatively well on VizWiz (Gurari et al. 2018)—likely due to its early-stage pruning in low-quality images—its advantage diminishes as the token retention decreases.

### Ablation Studies

**Effect of Modules.** We report performance on POPE (Li et al. 2023) and VQA<sup>Text</sup> (Singh et al. 2019) under a 22.2% token reduction setting. Each row in Table 2 represents a different combination of components within our framework. The results demonstrate that all individual modules contribute positively to performance. Specifically, incorporating visual-only scoring—by removing dependence on text queries within the LLM—yields a notable improvement. Visual encoder pruning offers substantial gains by eliminating redundant tokens early in the pipeline, improving efficiency without compromising essential information. Additionally, the inclusion of stage-wise token merging further boosts performance by retaining fine-grained visual context that would otherwise be lost. Together, these findings highlight the effectiveness and complementary nature of each component in enhancing model performance under constrained token budgets.

### Conclusion

In this work, we introduce VisionDrop, a simple yet effective training-free, visual-only pruning framework designed to mitigate modality misalignment and reduce computational cost in LVLMs. By treating the visual encoder and the LLM as a unified processing pipeline, VisionDrop performs progressive dominant token selection and contextual merging without relying on text-conditioned signals. This design allows the model to preserve critical visual cues under strict

token budgets. Moreover, VisionDrop’s reliance on purely visual signals makes it especially advantageous in domains where language cues are sparse or weakly aligned with visual content, such as high-resolution medical or remote sensing images.

### References

- Bai, J.; Bai, S.; Chu, Y.; Cui, Z.; Dang, K.; Deng, X.; et al. 2023. Qwen Technical Report. *arXiv preprint arXiv:2309.16609*.
- Bai, S.; Chen, K.; Liu, X.; Wang, J.; Ge, W.; Song, S.; et al. 2025. Qwen2.5-VL Technical Report. *arXiv preprint arXiv:2502.13923*.
- Bolya, D.; Fu, C.-Y.; Dai, X.; Zhang, P.; Feichtenhofer, C.; and Hoffman, J. 2023. Token Merging: Your ViT But Faster. In *ICLR*.
- Cai, Z.; Cao, M.; Chen, H.; Chen, K.; Chen, K.; Chen, X.; et al. 2024. InternLM2 Technical Report. *arXiv preprint arXiv:2403.17297*.
- Chen, G.; Shen, L.; Shao, R.; Deng, X.; and Nie, L. 2024a. LION : Empowering Multimodal Large Language Model with Dual-Level Visual Knowledge. In *CVPR*, 26530–26540.
- Chen, L.; Zhao, H.; Liu, T.; Bai, S.; Lin, J.; Zhou, C.; and Chang, B. 2024b. An Image is Worth 1/2 Tokens After Layer 2: Plug-and-Play Inference Acceleration for Large Vision-Language Models. In *ECCV*.
- Chen, Y.; Xue, F.; Li, D.; Hu, Q.; Zhu, L.; Li, X.; et al. 2025a. LongVILA: Scaling Long-Context Visual Language Models for Long Videos. In *ICLR*.
- Chen, Z.; Wang, W.; Cao, Y.; Liu, Y.; Gao, Z.; Cui, E.; et al. 2025b. Expanding Performance Boundaries of Open-Source Multimodal Models with Model, Data, and Test-Time Scaling. *arXiv preprint arXiv:2412.05271*.
- Fu, C.; Chen, P.; Shen, Y.; Qin, Y.; Zhang, M.; Lin, X.; et al. 2024. MME: A Comprehensive Evaluation Benchmark for Multimodal Large Language Models. *arXiv preprint arXiv:2306.13394*.
- Goyal, Y.; Khot, T.; Summers-Stay, D.; Batra, D.; and Parikh, D. 2017. Making the V in VQA Matter: Elevating the Role of Image Understanding in Visual Question Answering. In *CVPR*, 6325–6334.
- Gurari, D.; Li, Q.; Stangl, A. J.; Guo, A.; Lin, C.; Grauman, K.; Luo, J.; and Bigham, J. P. 2018. VizWiz Grand Challenge: Answering Visual Questions From Blind People. In *CVPR*, 3608–3617.
- Hudson, D. A.; and Manning, C. D. 2019. GQA: A New Dataset for Real-World Visual Reasoning and Compositional Question Answering. In *CVPR*, 6700–6709.
- Jiang, A. Q.; Sablayrolles, A.; Mensch, A.; Bamford, C.; Chaplot, D. S.; de las Casas, D.; et al. 2023. Mistral 7B. *arXiv preprint arXiv:2310.06825*.
- Li, B.; Zhang, Y.; Guo, D.; Zhang, R.; Li, F.; Zhang, H.; Zhang, K.; Li, Y.; Liu, Z.; and Li, C. 2024. LLaVA-OneVision: Easy Visual Task Transfer. *arXiv preprint arXiv:2408.03326*.

- Li, Y.; Du, Y.; Zhou, K.; Wang, J.; Zhao, W. X.; and Wen, J. 2023. Evaluating Object Hallucination in Large Vision-Language Models. In *EMNLP*, 292–305. Association for Computational Linguistics.
- Liu, H.; Li, C.; Li, Y.; and Lee, Y. J. 2024a. Improved Baselines with Visual Instruction Tuning. In *CVPR*, 26286–26296.
- Liu, H.; Li, C.; Li, Y.; Li, B.; Zhang, Y.; Shen, S.; and Lee, Y. J. 2024b. LLaVA-NeXT: Improved reasoning, OCR, and world knowledge.
- Liu, H.; Li, C.; Wu, Q.; and Lee, Y. J. 2023. Visual Instruction Tuning. In *NeurIPS*.
- Liu, Y.; Duan, H.; Zhang, Y.; Li, B.; Zhang, S.; Zhao, W.; Yuan, Y.; Wang, J.; He, C.; Liu, Z.; Chen, K.; and Lin, D. 2024c. MMBench: Is Your Multi-modal Model an All-Around Player? In *ECCV*, volume 15064, 216–233.
- Lu, P.; Mishra, S.; Xia, T.; Qiu, L.; Chang, K.; Zhu, S.; Tafford, O.; Clark, P.; and Kalyan, A. 2022. Learn to Explain: Multimodal Reasoning via Thought Chains for Science Question Answering. In *NeurIPS*.
- Qwen; ; Yang, A.; Yang, B.; Zhang, B.; Hui, B.; Zheng, B.; Yu, B.; et al. 2025. Qwen2.5 Technical Report. *arXiv preprint arXiv:2412.15115*.
- Radford, A.; Kim, J. W.; Hallacy, C.; Ramesh, A.; Goh, G.; Agarwal, S.; Sastry, G.; Askell, A.; Mishkin, P.; Clark, J.; Krueger, G.; and Sutskever, I. 2021. Learning Transferable Visual Models From Natural Language Supervision. In *ICML*, volume 139, 8748–8763.
- Singh, A.; Natarajan, V.; Shah, M.; Jiang, Y.; Chen, X.; Batra, D.; Parikh, D.; and Rohrbach, M. 2019. Towards VQA Models That Can Read. In *CVPR*, 8317–8326.
- Team, G.; Mesnard, T.; Hardin, C.; Dadashi, R.; Bhupatiraju, S.; Pathak, S.; et al. 2024. Gemma: Open Models Based on Gemini Research and Technology. *arXiv preprint arXiv:2403.08295*.
- Tong, J.; Jin, W.; Qin, P.; Li, A.; Zou, Y.; Li, Y.; Li, Y.; and Li, R. 2025. FlowCut: Rethinking Redundancy via Information Flow for Efficient Vision-Language Models. *arXiv preprint arXiv:2505.19536*.
- Touvron, H.; Lavril, T.; Izacard, G.; Martinet, X.; Lachaux, M.-A.; Lacroix, T.; et al. 2023. LLaMA: Open and Efficient Foundation Language Models. *arXiv preprint arXiv:2302.13971*.
- Vaswani, A.; Shazeer, N.; Parmar, N.; Uszkoreit, J.; Jones, L.; Gomez, A. N.; Kaiser, L.; and Polosukhin, I. 2017. Attention is All you Need. In *NeurIPS*, 5998–6008.
- Wang, P.; Bai, S.; Tan, S.; Wang, S.; Fan, Z.; Bai, J.; et al. 2024. Qwen2-VL: Enhancing Vision-Language Model’s Perception of the World at Any Resolution. *arXiv preprint arXiv:2409.12191*.
- Xing, L.; Huang, Q.; Dong, X.; Lu, J.; Zhang, P.; Zang, Y.; Cao, Y.; He, C.; Wang, J.; Wu, F.; and Lin, D. 2025. PyramidDrop: Accelerating Your Large Vision-Language Models via Pyramid Visual Redundancy Reduction. In *CVPR*.
- Yang, S.; Chen, Y.; Tian, Z.; Wang, C.; Li, J.; Yu, B.; and Jia, J. 2025. VisionZip: Longer is Better but Not Necessary in Vision Language Models. In *CVPR*.
- Zhai, X.; Mustafa, B.; Kolesnikov, A.; and Beyer, L. 2023. Sigmoid Loss for Language Image Pre-Training. In *ICCV*, 11941–11952.
- Zhang, C.; Ma, K.; Fang, T.; Yu, W.; Zhang, H.; Zhang, Z.; Xie, Y.; Sycara, K.; Mi, H.; and Yu, D. 2025a. VScan: Rethinking Visual Token Reduction for Efficient Large Vision-Language Models. *arXiv preprint arXiv:2505.22654*.
- Zhang, P.; Zhang, K.; Li, B.; Zeng, G.; Yang, J.; Zhang, Y.; et al. 2024. Long Context Transfer from Language to Vision. *arXiv preprint arXiv:2406.16852*.
- Zhang, Q.; Liu, M.; Li, L.; Lu, M.; Zhang, Y.; Pan, J.; She, Q.; and Zhang, S. 2025b. Beyond Attention or Similarity: Maximizing Conditional Diversity for Token Pruning in MLLMs. *arXiv preprint arXiv:2506.10967*.
- Zhang, Y.; Fan, C.-K.; Ma, J.; Zheng, W.; Huang, T.; Cheng, K.; Gudovskiy, D.; Okuno, T.; Nakata, Y.; Keutzer, K.; et al. 2025c. SparseVLM: Visual Token Sparsification for Efficient Vision-Language Model Inference. In *ICML*.
- Zhu, J.; Wang, W.; Chen, Z.; Liu, Z.; Ye, S.; Gu, L.; et al. 2025. InternVL3: Exploring Advanced Training and Test-Time Recipes for Open-Source Multimodal Models. *arXiv preprint arXiv:2504.10479*.